Int. J. High Technology Ceramics 1 (1985) 129–137

Crack Propagation Resistance of Aluminium Titanate Ceramics

Kenya Hamano, Yutaka Ohya and Zenbe-e Nakagawa

Research Laboratory of Engineering Materials, Tokyo Institute of Technology, 4259 Nagatsuta, Midori-ku, Yokohama-shi 227, Japan

SUMMARY

The crack propagation behaviour of aluminium titanate ceramics containing grain boundary microcracks has been investigated. The mean grain size of the aluminium titanate was 0·6 μm at 1300°C and 2·3 μm at 1500°C. Specimens sintered at 1450 and 1500°C contained grain boundary microcracks, while the specimen sintered at 1300°C had few cracks. Grain boundary microcracks decreased the bend strength and Young's modulus of the specimens. At the propagation of a crack, the microcracks deflected and caused branching of the crack, and blunted the crack tip; consequently, work of fracture of the specimen increased to more than twice the original value and crack propagation velocity decreased to 1/2000 of that in a microcrack-free aluminium titanate ceramic.

1. INTRODUCTION

Aluminium titanate ceramics are well known as low thermal expansion materials but have the disadvantage of low mechanical strength.[1,2] These two characteristics are due to grain boundary microcracks caused by a marked anisotropy of the thermal expansion of the aluminium titanate crystal.[1,3] In order to improve the mechanical strength, it is widely appreciated that a decrease in the size of cracks at the grain boundaries is necessary. In single-phase non-cubic polycrystalline ceramics, grain boundary microcracking occurs during the cooling period after sintering, under a set of conditions which is determined by their microstructure, thermal expansion anisotropy, fracture surface energy,

Int. J. High Technology Ceramics 0267-3762/85/$03·30

elastic moduli, and the difference between their sintering temperatures and room temperature.[4-6]

As aluminium titanate has a high thermal expansion anisotropy, in order to reduce the grain boundary microcracking, its grain size must be decreased markedly. Cleveland and Bradt[6] estimated that the 'transition grain size' for microcracking in aluminium titanate ceramics was 1–2 μm. One of the results of our study on the improvement of the mechanical strength of the aluminium titanate ceramics[7-10] showed that the transition grain size is 2·5 μm,[8] and that the bend strength of the sintered specimens increased suddenly as the grain size became smaller than this value.

Recently, several methods of toughening ceramic materials have been investigated; microcrack toughening[11-13] is one of these. Many researchers use K_{Ic} and the work of fracture to evaluate the toughness of the ceramic materials. In addition to these, the crack propagation velocity during fracture would be thought to be one of the significant evaluating factors. Although the crack velocity in fatigue fracture and slow crack growth has been measured, the fast crack velocity occurring during fracture has seldom been measured, because of the difficulties in making the measurement,[14] especially for opaque specimens.[15] Thus discussion of the relationship between crack velocity during fracture of the specimens and their microstructure has been rare.

In this paper the relationship between the microstructure of the aluminium titanate ceramics and their behaviour during fracture, i.e. crack propagation phenomena, crack velocity during fracture and work of fracture, has been investigated.

2. EXPERIMENTAL PROCEDURE

The sintered specimens were prepared from synthesized aluminium titanate powder having a mean particle size of $\sim 0{\cdot}5\,\mu$m and containing ~ 5 wt% aluminium oxide contaminant introduced during its ball-milling. Sintering temperatures were 1300, 1350, 1400, 1450 and 1500 °C, and the sintering period was 4 h. Thermal contraction and expansion of the specimens during the cooling period were measured by a non-loading type dilatometer.[16] Bend strengths were measured by the 3-point loading method, and the results were shown as the mean value of three specimens for each sintering condition. The microstructure and appearance of the side surfaces of the specimens after the bend test were observed using a scanning electron microscope. Work of fracture was determined, using a single-edge notched-beam specimen, by 3-point loading. The notch width was $\sim 0{\cdot}2$ mm and its

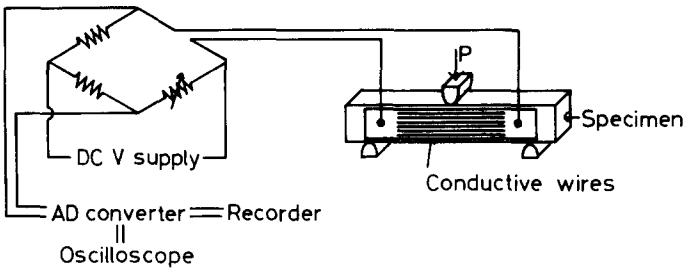

Fig. 1. Schematic diagram showing the experimental arrangement for measurement of crack velocity.

depth was ~ 40 % of the specimen thickness. Bulk density of the sintered specimens was measured by the mercury displacement method.

Crack propagation velocity during the fracture was determined as follows. Conductive wires which were connected to terminals at both sides were printed on a side surface of the sintered specimen and then baked. The width of each printed wire was ~ 0·2 mm, and the distance between each wire was also ~ 0·2 mm. When the crack propagates during fracture, it cuts the printed wires, and the electrical resistance between the terminals is increased. This change of resistance was transformed to a voltage by means of a Wheatstone bridge, and was then recorded as a function of time. The very rapid change in voltage required the use of an ultra-high-speed A–D converter with a digital memory (Transient Converter TCG-4000S, Riken Denshi Co., Ltd). This equipment has a maximum resolution of 0·05 μs/word and can memorize 4096 words. A schematic diagram of the experimental arrangement for measurement of the crack velocity is shown in Fig. 1.

3. RESULTS AND DISCUSSION

3.1. Grain boundary cracking and microstructure

During cooling subsequent to sintering, grain boundary cracking occurs, due to the high thermal expansion anisotropy of the aluminium titanate, and this cracking causes expansion of the specimens.[17] Figure 2 shows the thermal contraction and expansion curves of the specimens during cooling from their sintering temperatures. Every specimen changed from a contraction to an expansion at temperatures in the range 300–200 °C. The specimen sintered at 1400 °C expanded ~ 1 %, the largest value in this set of experiments. Specimens sintered at 1350, 1450 and 1500 °C expanded by ~ 0·3–0·5 %; the specimen sintered at 1300 °C showed very little expansion.

Figure 3 shows the fractured surfaces of the sintered specimens. The mean grain size of the titanate increased from 0·6 μm following sintering at 1300 °C to 2·3 μm at 1500 °C. The specimen sintered at 1400 °C had large and

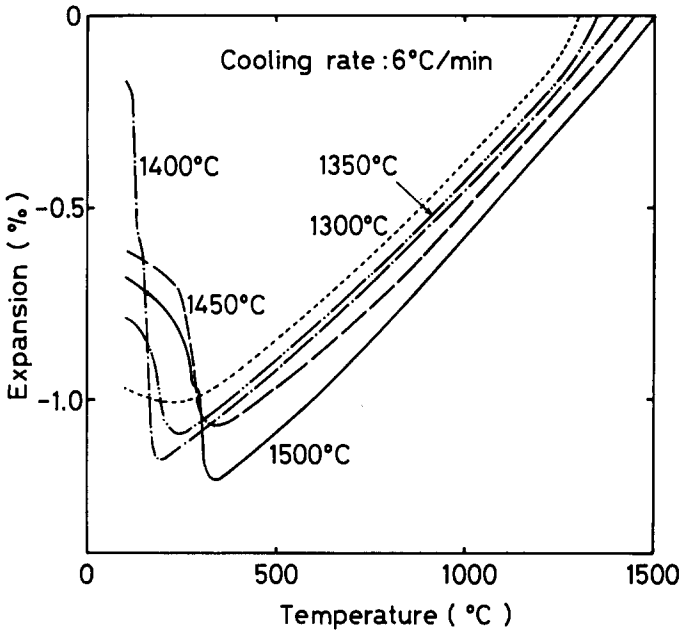

Fig. 2. Thermal contraction and expansion curves obtained during cooling from the sintering temperatures.

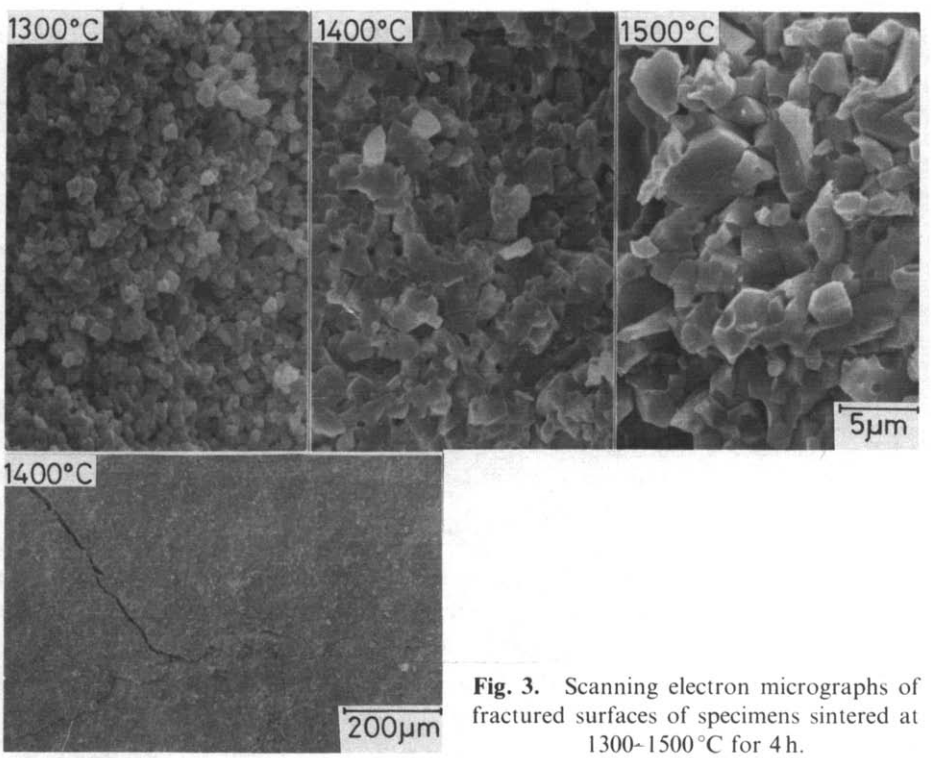

Fig. 3. Scanning electron micrographs of fractured surfaces of specimens sintered at 1300-1500 °C for 4 h.

continuous cracks through the body and failed when cooled to room temperature. Specimens sintered at 1450 and 1500 °C had small grain boundary microcracks and the microcracks of the 1450 °C specimen appeared to be continuous. The specimen sintered at 1300 °C had few cracks. The degree of microcracking and the size of the cracks in the sintered specimens can be seen to correspond with the degree of expansion during cooling.

3.2. Mechanical properties of sintered specimens

Bend strengths and bulk densities of the sintered bodies are shown in Fig. 4. The specimen sintered at 1400 °C had already fractured during cooling, so the bend strength of this specimen was considered as 0 MPa. The specimen sintered at 1300 °C, which contained few cracks, showed the highest strength. The specimens sintered at 1350 and 1450 °C were weak because the cracks in these specimens were comparatively large and continuous. From these results it becomes clear that a continuous crack is more harmful than discrete isolated microcracks and has the effect of lowering the strength of the specimens.

The microcracks present on the grain boundary also influenced the stress–strain relationship of the specimen, which is shown in Fig. 5. The specimen sintered at 1300 °C showed a linear stress–strain relation, whereas the specimens sintered at 1450 and 1500 °C did not show such behaviour and fractured in a more stable manner. From the initial straight part of the stress–strain curves, the Young's modulus was calculated and this is also

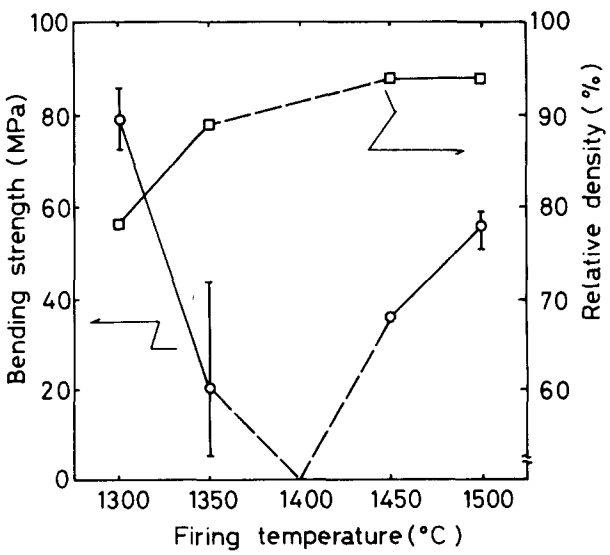

Fig. 4. Bend strengths and bulk densities of sintered specimens.

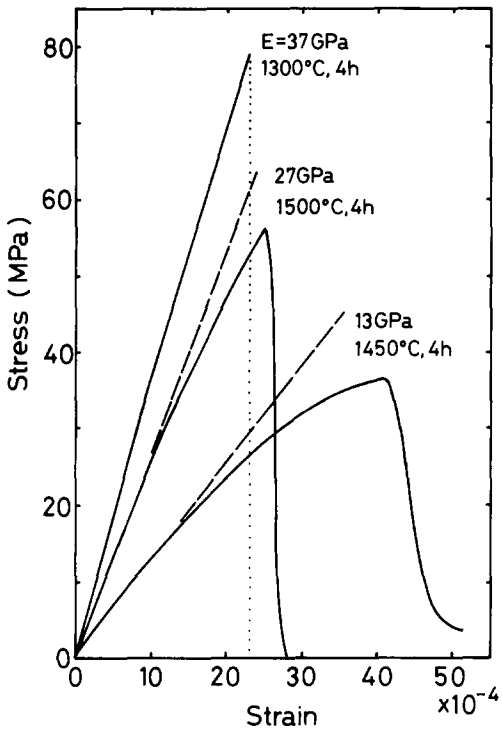

Fig. 5. Stress–strain curves obtained in 3-point bending.

shown in Fig. 5. The specimen sintered at 1300 °C has a higher modulus than the others, which whilst denser, contained appreciable amounts of cracks on their grain boundaries. This decrease in Young's modulus of the specimens containing grain boundary microcracks would be caused by the decrease in the area of contact across the sintered grain boundaries.

The microcracks also affected the fracture behaviour of the specimens. After the bend test, the specimens sintered at 1450 and 1500 °C did not break into separate pieces (Fig. 6(a)). In these specimens, as shown on scanning electron micrographs of their side surfaces in Fig. 6(b), cracks were deflected, branched, and blunted by the grain boundary microcracks and these processes finally combined to stop further propagation.

3.3. Work of fracture and crack propagation velocity during fracture

The work of fracture of the specimens sintered at 1300 and 1450 °C was measured. In this measurement both specimens were fractured in a stable manner. The work of fracture, γ_{wof}, was calculated to be $16{\cdot}8 \pm 0{\cdot}3$ and $38{\cdot}6 \pm 3{\cdot}1\ \mathrm{Jm}^{-2}$ for specimens sintered at 1300 and 1450 °C, respectively. This result indicates that the presence of the grain boundary microcracks in the specimen sintered at 1450 °C increases the work of fracture.

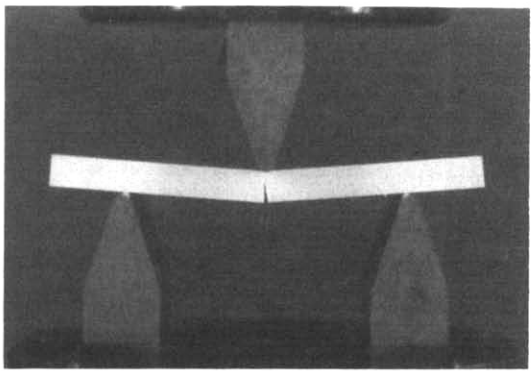

(a)

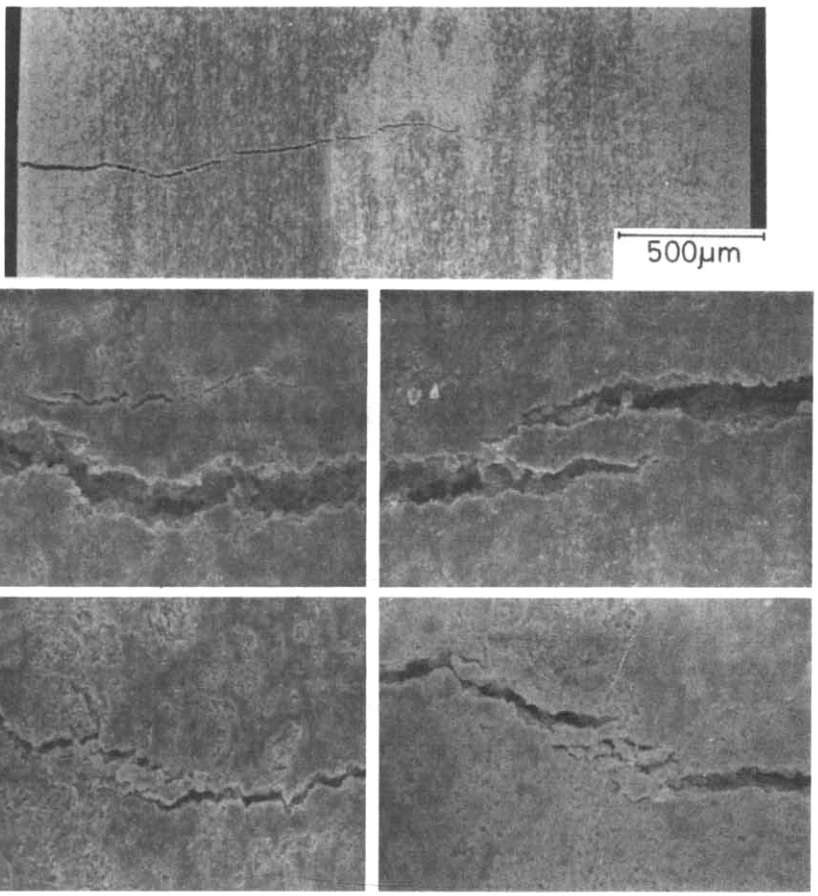

(b)

Fig. 6. Specimen fracture (a) and the side surface (b) of the specimen sintered at 1450 °C, after the bend test.

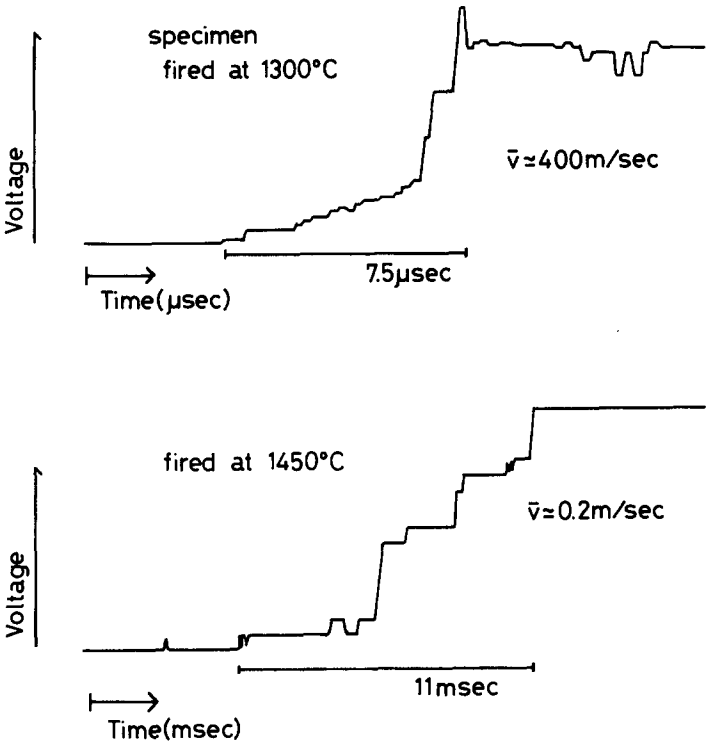

Fig. 7. Voltage–time relationships obtained during fracture, used to determine crack velocity.

Figure 7 shows voltage changes between two terminals printed on the side surface of the specimens sintered at 1300 and 1450 °C during fracture in the bend test. From this graph mean velocities of crack propagation were determined. The velocities were calculated to be ~ 400 and $0{\cdot}2\ \mathrm{m\ s^{-1}}$ for the specimens sintered at 1300 and 1450 °C, respectively. A fast crack extension speed of $400\ \mathrm{m\ s^{-1}}$ is a value comparable with that reported for hot-pressed silicon nitride[15] and other dense ceramics. The microcracks on the grain boundaries in aluminium titanate thus decrease the crack propagation velocity to 1/2000 of the velocity for microcrack-free specimens.

These measurements of the crack propagation velocity and the change in value of the work of fracture give a strong indication that the grain boundary microcracks interfere significantly with the crack extension.

4. CONCLUSION

Microcracks on the grain boundaries of the aluminium titanate studied decrease the bend strength and Young's modulus of the specimens by linking

with a critical crack and by reducing the area of contact between boundaries. However, these microcracks increase the resistance to crack propagation on fracture by mechanisms involving crack deflection, branching and blunting.

REFERENCES

1. Buessem, W. R., Thielke, N. R. and Sarakauskas, R. V., *Ceramic Age*, **60** (1952) 38.
2. Hamano, K., *Taikabutsu* [*Refractories*], **27** (1975) 520.
3. Morosin, B. and Lynch, R. W., *Acta Cryst.*, **B28** (1972) 1040.
4. Davidge, R. W., *Acta Met.*, **29** (1981) 1695.
5. Rice, R. W. and Pohanka, R. C., *J. Am. Ceram. Soc.*, **62** (1979) 559.
6. Cleveland, J. J. and Bradt, R. C., *ibid.*, **61** (1978) 478.
7. Hamano, K., Ohya, Y. and Nakagawa, Z., *Yogyo-Kyokai-Shi*, **91** (1983) 289.
8. Ohya, Y., Hamano, K. and Nakagawa, Z. *ibid.*, **91** (1983) 289.
9. Hamano, K., Nakagawa, Z., Sawano, K. and Hasegawa, M., *Nippon Kagaku Kaishi*, (1981) 1647.
10. Qian, D., Ohya, Y., Hamano, K. and Nakagawa, Z., *Yogyo-Kyokai-Shi*, **93** (1985) 315.
11. Green, D. J., Nicholson, P. S. and Embury, J. D., *J. Am. Ceram. Soc.*, **56** (1973) 619.
12. Evans, A. G. and Faber, K. T., *ibid.*, **64** (1981) 394.
13. Evans, A. G. and Faber, K. T., *ibid.*, **67** (1984) 255.
14. Schardin, H. and Struth, W., *Glastech. Ber.*, **16** (1938) 219.
15. Matsunaga, K., Takahira, K., Isobe, T. and Hashimoto, R., *Yogyo-Kyokai-Shi*, **90** (1982) 333.
16. Hamano, K., *Taikabutsu* [*Refractories*], **36** (1984) 231.
17. Wright, R. E., *J. Am. Ceram. Soc.*, **55** (1972) 54.

Received 10 April 1985; amended version received and accepted 31 October 1985